Nonlinear analysis of rectangular concrete-filled double steel tubular short columns incorporating local buckling

Figures and tables

Table 1 Comparison of predicted and experimental ultimate axial loads of square CFDST short columns.

Specimen	Outer Tube			Inner Tube			Concrete		Ultimate axial load			Ref.
	$B_o \times D_o \times t_o$ (mm)	$\frac{D_o}{t_o}$	f_{syo} (MPa)	$D_i \times t_i$ (mm)	$\frac{D_i}{t_i}$	f_{syi} (MPa)	f'_{co} (MPa)	f'_{ci} (MPa)	$P_{u,\exp}$ (kN)	$P_{u,num}$ (kN)	$\frac{P_{u,num}}{P_{u,\exp}}$	
I-CSCFT1	180×180×3.62	49.7	348	89×2.6	34.2	314	89.85	74.38	3643	3436	0.94	[19]
I-CSCFT2	180×180×3.62	49.7	348	89×3.32	26.8	324	89.85	74.38	3583	3487	0.97	
I-CSCFT4	180×180×3.62	49.7	348	114×4.56	25.0	322	89.85	74.38	3820	3707	0.97	
I-CSCFT5	180×180×3.62	49.7	348	140×2.84	49.3	345	89.85	74.38	3940	3541	0.90	
I-CSCFT7	180×180×5.4	33.3	338	89×2.6	34.2	314	89.85	74.38	3865	3784	0.98	
I-CSCFT8	180×180×5.4	33.3	338	89×3.32	26.8	324	89.85	74.38	3947	3836	0.97	
I-CSCFT9	180×180×5.4	33.3	338	114×3.35	34.0	328	89.85	74.38	4045	3976	0.98	
I-CSCFT10	180×180×5.4	33.3	338	114×4.56	25.0	322	89.85	74.38	4121	4063	0.99	
I-CSCFT11	180×180×5.4	33.3	338	140×2.84	49.3	345	89.85	74.38	4251	3874	0.91	
I-CSCFT12	180×180×5.4	33.3	338	140×3.97	35.3	308	89.85	74.38	4258	4147	0.97	
II-CSCFT1	180×180×3.62	49.7	348	89×2.6	34.2	314	74.38	89.85	3355	3186	0.95	
II-CSCFT2	180×180×3.62	49.7	348	114×3.35	34.0	328	74.38	89.85	3686	3493	0.95	
II-CSCFT4	180×180×5.4	33.3	338	89×2.6	34.2	314	74.38	89.85	3814	3553	0.93	
II-CSCFT5	180×180×5.4	33.3	338	114×3.35	34.0	328	74.38	89.85	4043	3867	0.96	
II-CSCFT6	180×180×5.4	33.3	338	140×3.97	35.3	308	74.38	89.85	4428	4172	0.94	
II-CSCFT7	180×180×5.4	33.3	338	89×3.32	26.8	324	74.38	89.85	3855	3601	0.93	
III-CSCFT1	180×180×3.62	49.7	348	89×2.6	34.2	314	74.38	74.38	3198	3096	0.97	
III-CSCFT2	180×180×3.62	49.7	348	114×3.35	34.0	328	74.38	74.38	3415	3343	0.98	
III-CSCFT3	180×180×3.62	49.7	348	140×3.97	35.3	308	74.38	74.38	4120	3588	0.87	
III-CSCFT4	180×180×5.4	33.3	338	89×2.6	34.2	314	74.38	74.38	4021	3463	0.86	
III-CSCFT5	180×180×5.4	33.3	338	114×3.35	34.0	328	74.38	74.38	4165	3716	0.89	
III-CSCFT6	180×180×5.4	33.3	338	140×3.97	35.3	308	74.38	74.38	4436	3965	0.89	
III-CSCFT7	180×180×5.4	33.3	338	89×3.32	26.8	324	74.38	74.38	3900	3515	0.90	
SDS1-40a	200×200×2.01	99.5	230	136.5×1.94	70.4	492.1	43.44	43.44	2450	2379	0.97	[20]
SDS1-40b	200×200×2.01	99.5	230	136.5×1.94	70.4	492.1	43.44	43.44	2383	2379	1.00	
SDS1-70a	200×200×2.01	99.5	230	136.5×1.94	70.4	492.1	43.44	67.83	2997	2728	0.91	
SDS1-70b	200×200×2.01	99.5	230	136.5×1.94	70.4	492.1	43.44	67.83	2806	2728	0.97	
SDS2-40a	200×200×2.01	99.5	230	114.6×3.93	29.2	377.1	43.44	43.44	2366	2429	1.03	
SDS2-40b	200×200×2.01	99.5	230	114.6×3.93	29.2	377.1	43.44	43.44	2463	2429	0.99	
SDS2-70a	200×200×2.01	99.5	230	114.6×3.93	29.2	377.1	43.44	67.83	2765	2659	0.96	
SDS2-70b	200×200×2.01	99.5	230	114.6×3.93	29.2	377.1	43.44	67.83	2884	2659	0.92	
SDS3-40a	200×200×2.01	99.5	230	140.1×3.78	37.1	322.4	43.44	43.44	2505	2502	1.00	
SDS3-40b	200×200×2.01	99.5	230	140.1×3.78	37.1	322.4	43.44	43.44	2479	2502	1.01	
SDS3-70a	200×200×2.01	99.5	230	140.1×3.78	37.1	322.4	43.44	67.83	3144	2881	0.92	
SDS3-70b	200×200×2.01	99.5	230	140.1×3.78	37.1	322.4	43.44	67.83	3100	2881	0.93	
G1-2	120×120×2.6	46.2	407.5	58.5×1.4	41.8	352.5	29.92	29.92	980	946	0.97	[18]
G1-3	120×120×2.6	46.2	407.5	74×0.9	82.2	680	29.92	29.92	1040	1013	0.97	
G1-4	120×120×2.6	46.2	407.5	83×0.9	92.2	597	29.92	29.92	1080	1019	0.94	
Mean											0.95	
Standard Deviation (SD)											0.04	
Coefficients of Variance (COV)											0.04	

Table 2 Geometric and material properties of CFDST short columns used in the parameter study.

Column	Outer Tube			Inner Tube			Concrete	
	$B_o \times D_o \times t_o$ (mm)	D_o / t_o	f_{syo} (MPa)	$D_i \times t_i$ (mm)	D_i / t_i	f_{syi} (MPa)	f'_{co} (MPa)	f'_{ci} (MPa)
C1	450×450×12.8	35.2	350	-	-	-	-	70
C2	450×450×7.5	60	350	300×10	30	350	70	70
C3	450×450×7.5	60	350	150×10	15	350	70	70
C4	450×450×7.5	60	350	200×10	20	350	70	70
C5	450×450×7.5	60	350	250×10	25	350	70	70
C6	450×450×7.5	60	350	300×6.0	50	350	70	70
C7	450×450×7.5	60	350	300×7.5	40	350	70	70
C8	450×450×7.5	60	350	300×15	20	350	70	70
C9	200×200×2.01	99.5	492	136.5×1.94	70.4	492	35	35
C10	650×650×10	65	350	350×10	35	350	35	35
C11	650×650×10	65	350	350×10	35	350	50	50
C12	650×650×10	65	350	350×10	35	350	70	70
C13	650×650×10	65	350	350×10	35	350	90	90
C14	650×650×10	65	350	350×10	35	350	50	35
C15	650×650×10	65	350	350×10	35	350	50	50
C16	650×650×10	65	350	350×10	35	350	50	70
C17	650×650×10	65	350	350×10	35	350	50	90
C18	650×650×10	65	350	350×10	35	350	35	50
C19	650×650×10	65	350	350×10	35	350	50	50
C20	650×650×10	65	350	350×10	35	350	70	50
C21	650×650×10	65	350	350×10	35	350	90	50
C22	450×450×7.5	60	250	300×10	30	350	70	70
C23	450×450×7.5	60	350	300×10	30	350	70	70
C24	450×450×7.5	60	450	300×10	30	350	70	70
C25	450×450×7.5	60	520	300×10	30	350	70	70
C26	450×450×7.5	60	350	300×10	30	250	70	70
C27	450×450×7.5	60	350	300×10	30	350	70	70
C28	450×450×7.5	60	350	300×10	30	450	70	70
C29	450×450×7.5	60	350	300×10	30	520	70	70
C30	400×800×12	66.67	450	350×10	35	450	90	90
C31	600×800×12	66.67	450	350×10	35	450	90	90
C32	1000×800×12	66.67	450	350×10	35	450	90	90
C33	1200×800×12	66.67	450	350×10	35	450	90	90

Table 3 Comparison of ultimate strengths of rectangular CFDST short columns with the code predictions.

Specimen	$P_{u,\exp}$ (kN)	$P_{u,EC4}$ (kN)	$P_{u,ACi}$ (kN)	$P_{u,AISC}$ (kN)	$P_{u,AIJ}$ (kN)	$P_{u,des}$ (kN)	$\frac{P_{u,EC4}}{P_{u,\exp}}$	$\frac{P_{u,ACI}}{P_{u,\exp}}$	$\frac{P_{u,AISC}}{P_{u,\exp}}$	$\frac{P_{u,AIJ}}{P_{u,\exp}}$	$\frac{P_{u,des}}{P_{u,\exp}}$
I-CSCFT1	3643	3765	3263	3280	3703	3525	1.03	0.90	0.90	1.02	0.97
I-CSCFT2	3583	3852	3319	3334	3775	3599	1.08	0.93	0.93	1.05	1.00
I-CSCFT4	3820	4072	3440	3479	3937	3855	1.07	0.90	0.91	1.03	1.01
I-CSCFT5	3940	3911	3310	3392	3777	3541	0.99	0.84	0.86	0.96	0.90
I-CSCFT7	3865	4049	3556	3574	3980	3844	1.05	0.92	0.92	1.03	0.99
I-CSCFT8	3947	4138	3612	3628	4052	3917	1.05	0.92	0.92	1.03	0.99
I-CSCFT9	4045	4209	3635	3678	4087	4059	1.04	0.90	0.91	1.01	1.00
I-CSCFT10	4121	4364	3733	3772	4213	4173	1.06	0.91	0.92	1.02	1.01
I-CSCFT11	4251	4200	3603	3685	4054	3858	0.99	0.85	0.87	0.95	0.91
I-CSCFT12	4258	4321	3674	3752	4146	4199	1.01	0.86	0.88	0.97	0.99
II-CSCFT1	3355	3489	3025	3053	3423	3263	1.04	0.90	0.91	1.02	0.97
II-CSCFT2	3686	3760	3203	3261	3647	3588	1.02	0.87	0.88	0.99	0.97
II-CSCFT4	3814	3791	3334	3362	3718	3598	0.99	0.87	0.88	0.97	0.94
II-CSCFT5	4043	4067	3512	3570	3942	3923	1.01	0.87	0.88	0.98	0.97
II-CSCFT6	4428	4330	3680	3779	4153	4184	0.98	0.83	0.85	0.94	0.94
II-CSCFT7	3855	3879	3388	3414	3788	3662	1.01	0.88	0.89	0.98	0.95
III-CSCFT1	3198	3405	2953	2973	3338	3188	1.06	0.92	0.93	1.04	1.00
III-CSCFT2	3415	3625	3084	3130	3507	3461	1.06	0.90	0.92	1.03	1.01
III-CSCFT3	4120	3817	3191	3271	3646	3676	0.93	0.77	0.79	0.88	0.89
III-CSCFT4	4021	3709	3262	3283	3633	3524	0.92	0.81	0.82	0.90	0.88
III-CSCFT5	4165	3933	3393	3439	3802	3795	0.94	0.81	0.83	0.91	0.91
III-CSCFT6	4436	4126	3500	3580	3941	4010	0.93	0.79	0.81	0.89	0.90
III-CSCFT7	3900	3798	3318	3337	3705	3597	0.97	0.85	0.86	0.95	0.92
SDS1-40a	2450	2738	2235	2281	2589	2379	1.12	0.91	0.93	1.06	0.94
SDS1-40b	2383	2738	2235	2281	2589	2379	1.15	0.94	0.96	1.09	0.97
SDS1-70a	2997	3064	2522	2597	2926	2728	1.02	0.84	0.87	0.98	0.88
SDS1-70b	2806	3064	2522	2597	2926	2728	1.09	0.90	0.93	1.04	0.95
SDS2-40a	2366	2875	2327	2351	2707	2429	1.22	0.98	0.99	1.14	1.08
SDS2-40b	2463	2875	2327	2351	2707	2429	1.17	0.94	0.95	1.10	1.04
SDS2-70a	2765	3084	2512	2555	2925	2659	1.12	0.91	0.92	1.06	1.03
SDS2-70b	2884	3084	2512	2555	2925	2659	1.07	0.87	0.89	1.01	0.99
SDS3-40a	2505	2889	2324	2370	2705	2502	1.15	0.93	0.95	1.08	1.04
SDS3-40b	2479	2889	2324	2370	2705	2502	1.17	0.94	0.96	1.09	1.05
SDS3-70a	3144	3212	2610	2685	3041	2881	1.02	0.83	0.85	0.97	0.96
SDS3-70b	3100	3212	2610	2685	3041	2881	1.04	0.84	0.87	0.98	0.97
G1-2	980	1031	915	917	997	944	1.05	0.93	0.94	1.02	0.96
G1-3	1040	1124	969	976	1065	998	1.08	0.93	0.94	1.02	0.96
G1-4	1080	1122	968	978	1063	997	1.04	0.90	0.91	0.98	0.92
Mean							1.06	0.88	0.90	1.01	0.97
Standard Deviation (SD)							0.09	0.06	0.06	0.07	0.05
Coefficients of Variance (COV)							0.09	0.07	0.06	0.07	0.05

Table 4 Comparison of design ultimate strengths of CFDST columns with numerical predictions.

Column	$P_{u,des}$ (kN)	$P_{u,num}$ (kN)	$\frac{P_{u,des}}{P_{u,num}}$
C2	19376	19461	1.00
C3	16393	16894	0.97
C4	17368	17621	0.99
C5	18367	18462	0.99
C6	16835	17726	0.95
C7	18462	18787	0.98
C8	20897	20650	1.01
Mean			0.98
Standard Deviation (SD)			0.02
Coefficients of Variance (COV)			0.02

Table 5 Strength prediction formulas for rectangular CFDST short columns by design codes.

Design codes	Design equations
Eurocode 4 [5]	Circular CFST columns: $P_u = \eta_a A_s f_{sy} + A_c f_c (1 + \eta_c \frac{t}{D} \frac{f_{sy}}{f_c})$ $\eta_a = 0.25(3 + 2\bar{\lambda}) \quad (\eta_a \le 1.0)$ $\eta_c = 4.9 - 18.5\bar{\lambda} + 17\bar{\lambda}^2 \quad (\eta_c > 0)$ where the relative slenderness ratio is $\bar{\lambda} = \sqrt{\frac{N_{pl,Rk}}{N_{cr}}}$ Rectangular CFST columns: $P_u = A_s f_{sy} + A_c f_c^{'}$ Rectangular CFDST columns with inner circular tube: $P_{u,EC4} = A_{so} f_{syo} + A_{sc} f_c^{'} + \eta_a A_{si} f_{syi} + A_{cc} f_{cc} (1 + \eta_c \frac{t_i}{d_i} \frac{f_{syi}}{f_{ci}})$
ACI 318-11 [6]	$P_{u,ACI} = A_{so} f_{syo} + 0.85 A_{sc} f_{sc} + A_{si} f_{syi} + 0.85 A_{cc} f_{cc}$
AISC 360-16 [7]	$P_{u,AISC} = \begin{cases} P_o \left[0.658^{(P_o/P_e)} \right] & \text{for } P_e \ge 0.44 P_o \\ 0.877 P_e & \text{for } P_e < 0.44 P_o \end{cases}$ $P_o = A_{so} f_{syo} + C_2 A_{sc} f_{sc} + A_{si} f_{syi} + C_2 A_{cc} f_{cc}$ $P_e = \frac{\pi^2}{(KL)^2} (EI)_{eff}$ $(EI)_{eff} = E_{so} I_{so} + E_{si} I_{si} + C_4 E_{sc} I_{sc} + C_4 E_{cc} I_{cc}$ $C_4 = 0.6 + 2\left(\frac{A_s}{A_s + A_c} \right) \le 0.9$ $C_2 = \begin{cases} 0.95 & \text{for circular cross-section} \\ 0.85 & \text{for rectangular cross-section} \end{cases}$
AIJ [8]	$P_{u,AIJ} = A_{sc} f_{sc} + (1+\eta) A_{so} f_{syo} + + A_{cc} f_{cc} + (1+\eta) A_{si} f_{syi}$ $\eta = \begin{cases} 0.27 & \text{for circular cross-section} \\ 0 & \text{for rectangular cross-section} \end{cases}$

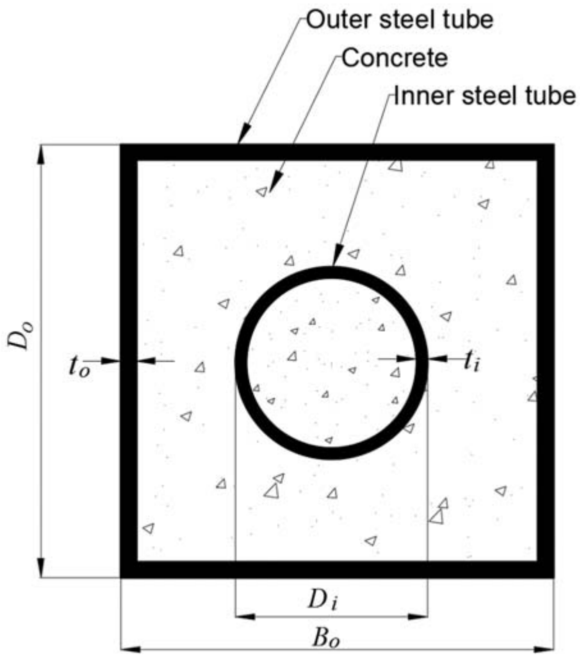

Fig. 1. Cross-section of rectangular CFDST column with inner circular steel tube.

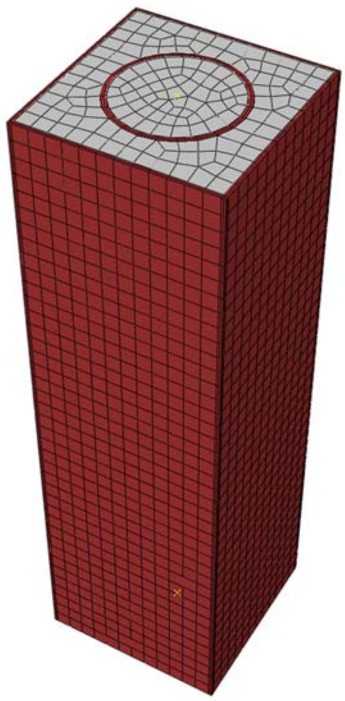

Fig. 2. Finite element model of CFDST column.

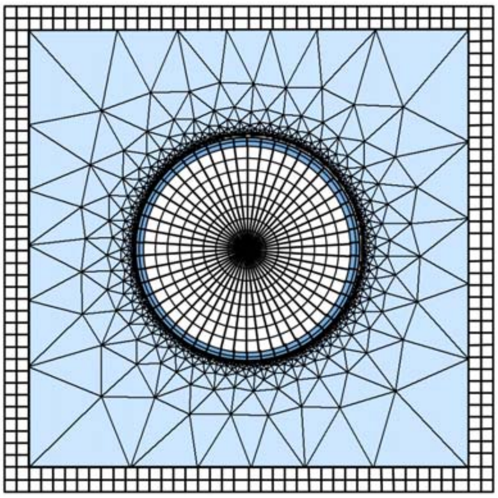

Fig. 3. Typical fiber mesh in CFDST column section with inner circular steel tube.

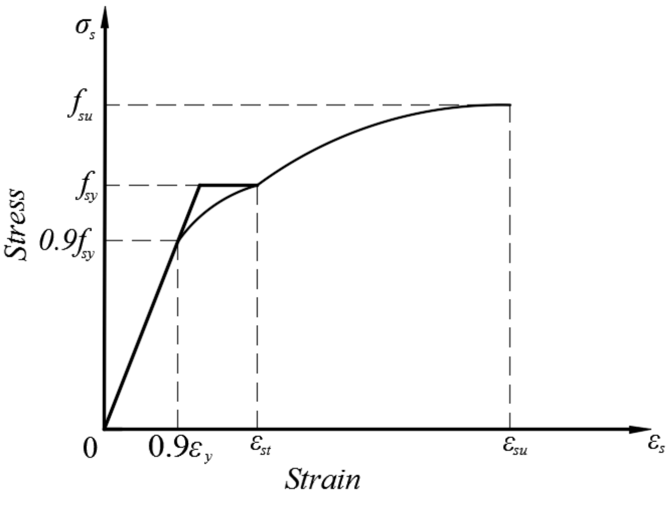

Fig. 4. Stress-strain curve for structural steel.

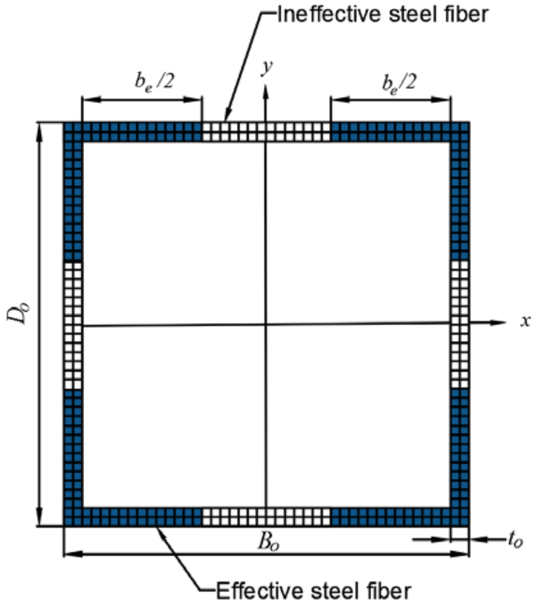

Fig. 5. Effective width of the outer rectangular steel tube.

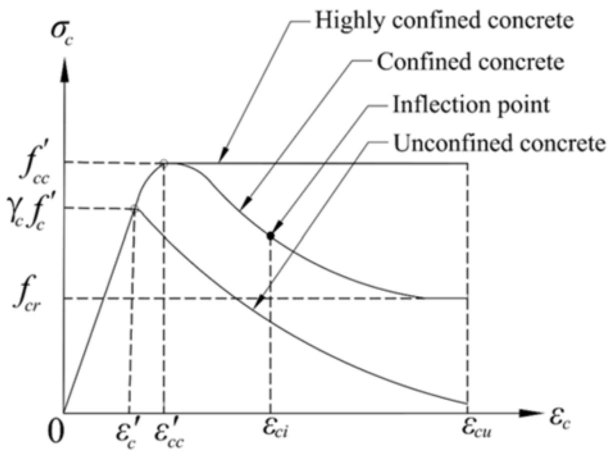

Fig. 6. Stress-strain curves for confined concrete in rectangular CFDST column.

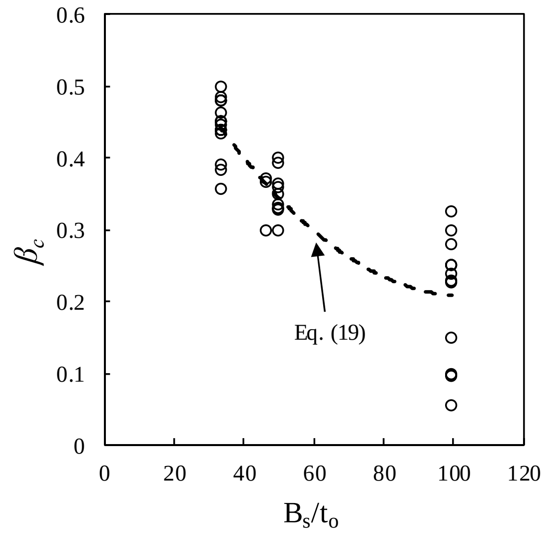

Fig. 7. Verification of the proposed expression for β_c .

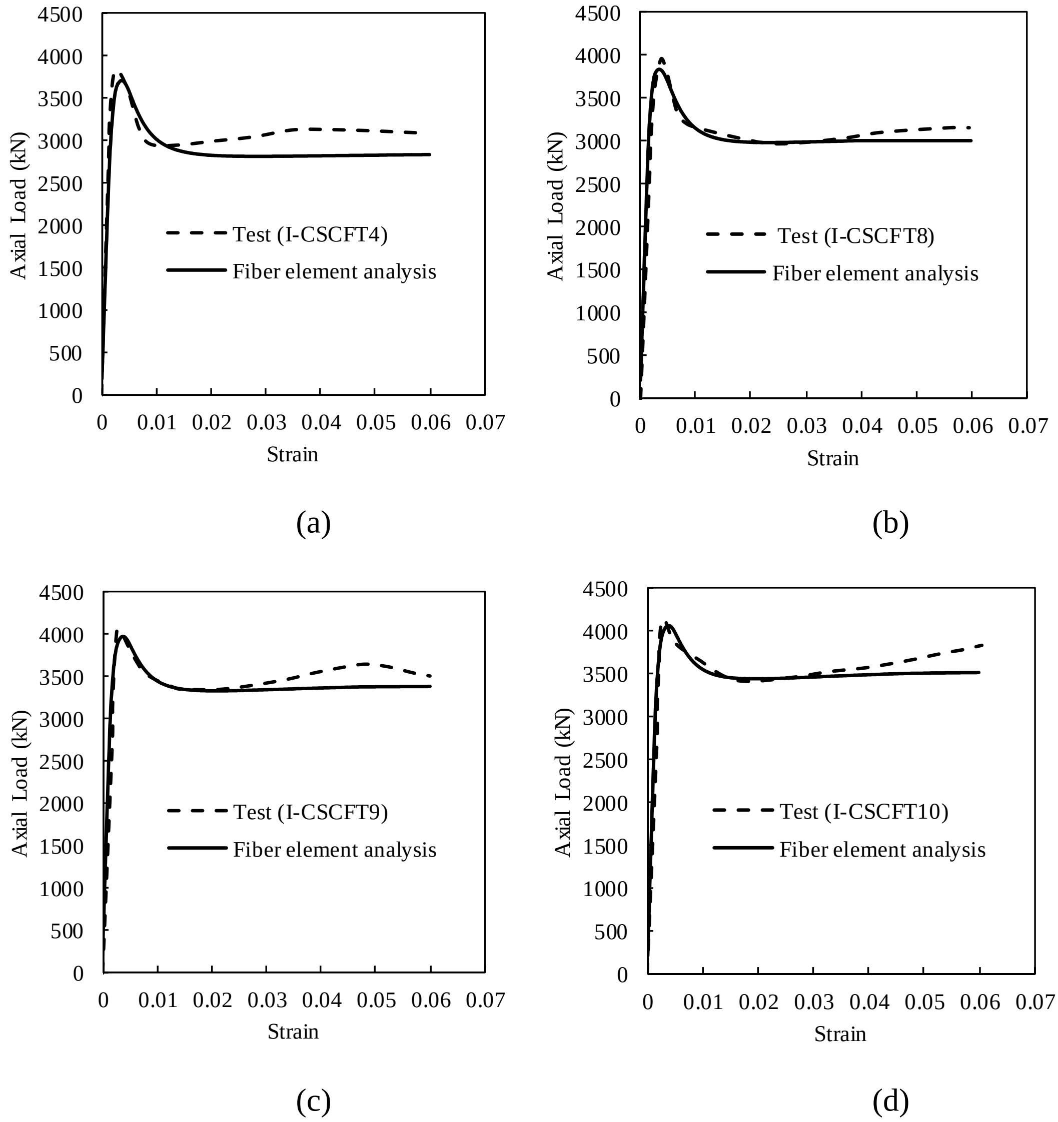

Fig. 8. Comparison of predicted and experimental axial load-strain curves of CFDST short columns tested by Qian et al. [19].

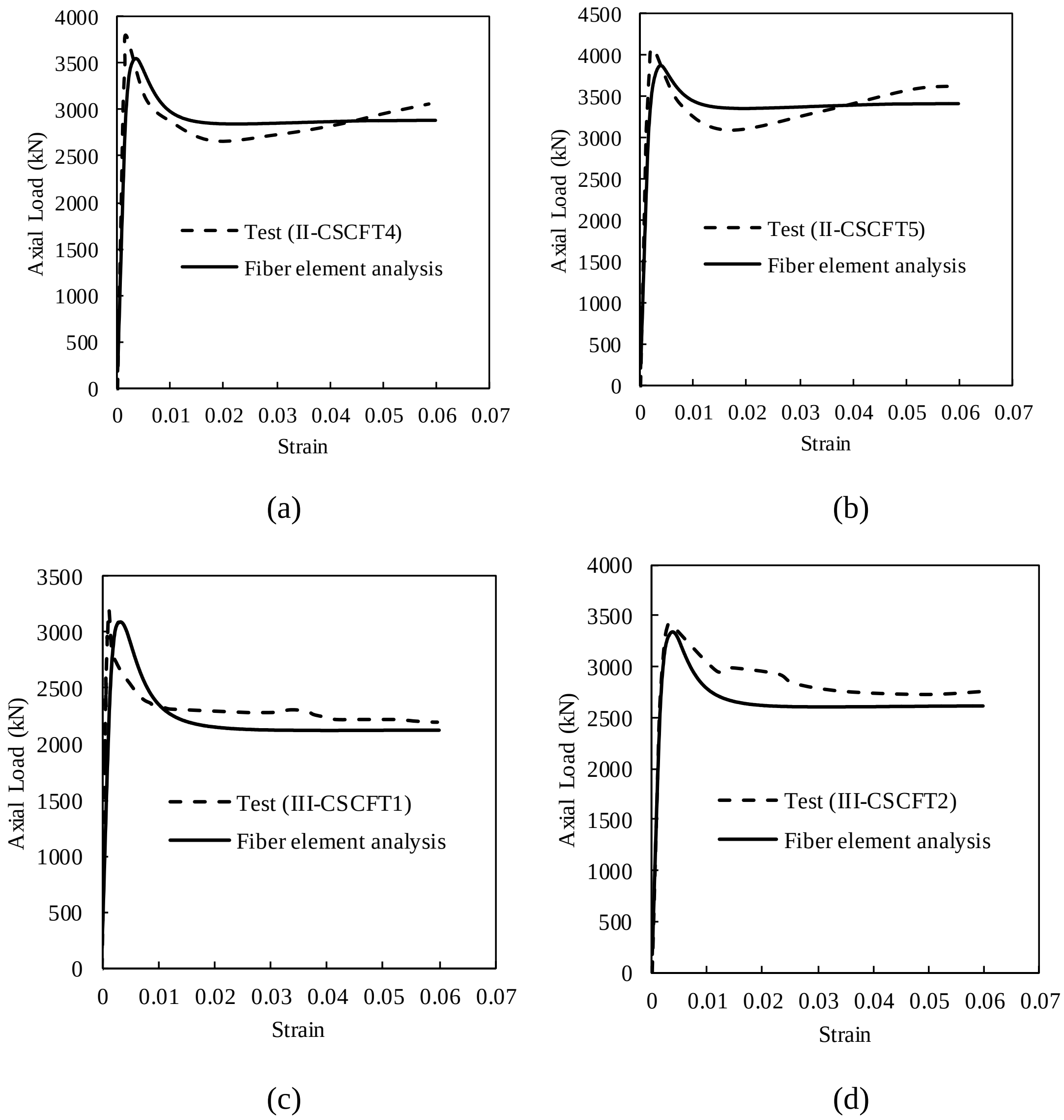

Fig. 9. Comparison of predicted and experimental axial load-strain curves of CFDST columns tested by Qian et al. [19].

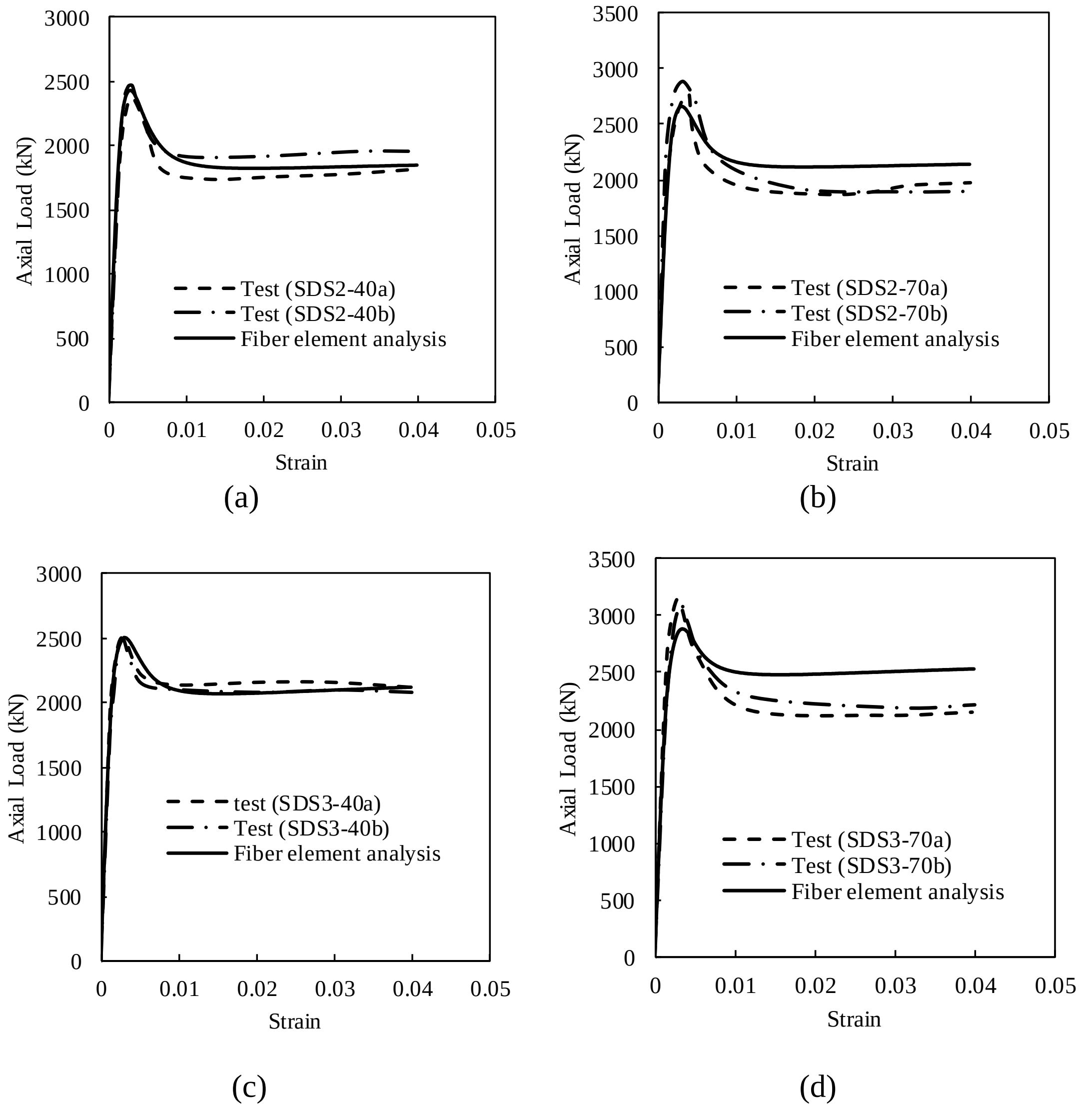

Fig. 10. Comparison of predicted and experimental axial load-strain curves of CFDST columns tested by Wang et al. [20].

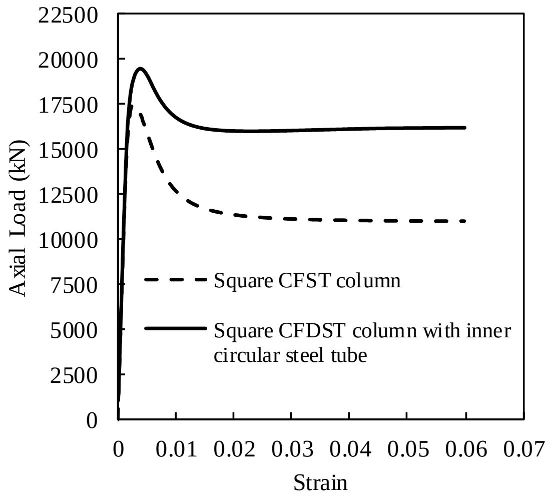

Fig. 11. Effects of the inner steel tube on the axial load-strain responses of CFDST short column.

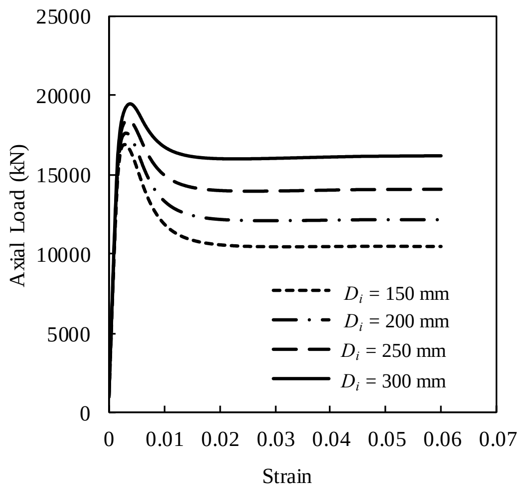

Fig. 12. Effects of the diameter of the inner steel tube on the axial load-strain responses of CFDST short columns.

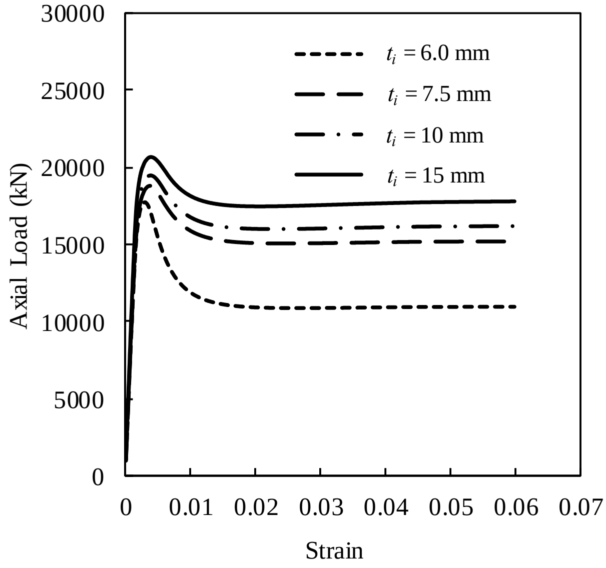

Fig. 13. Effects of the thickness of the inner steel tube on the axial load-strain responses of CFDST short columns.

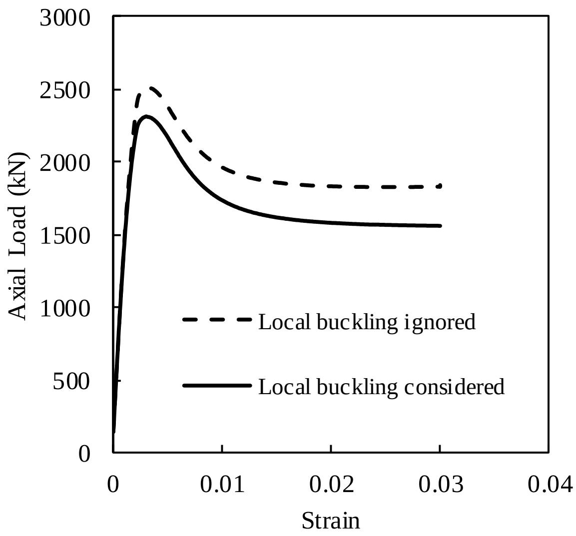

Fig. 14. Effects of local buckling of the outer steel tube on the axial load-strain responses of CFDST short columns.

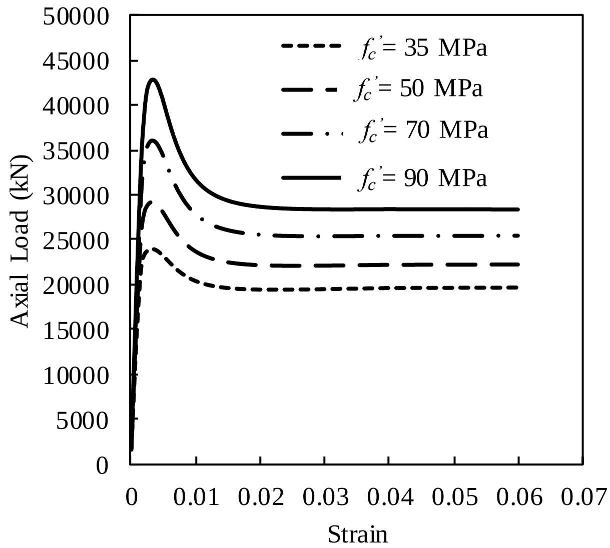

Fig. 15. Effects of concrete compressive strength on the axial load-strain responses of CFDST short columns.

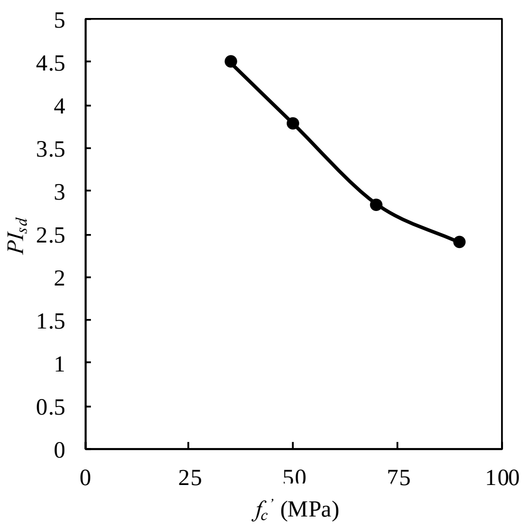

Fig. 16. Strain ductility indices of CFDST short columns with various concrete strengths.

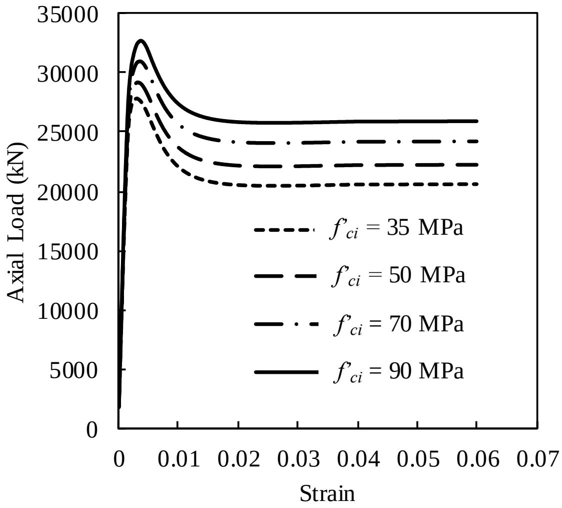

Fig. 17. Effects of core concrete compressive strength on the axial load-strain response of CFDST columns.

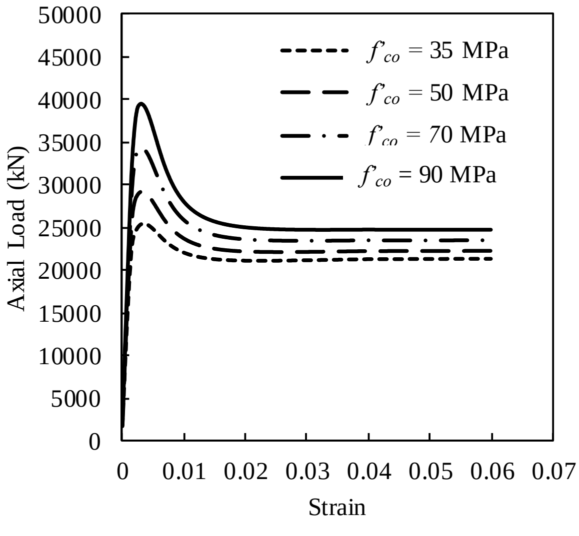

Fig. 18. Effects of sandwiched concrete compressive strength on the axial load-strain responses of CFDST columns.

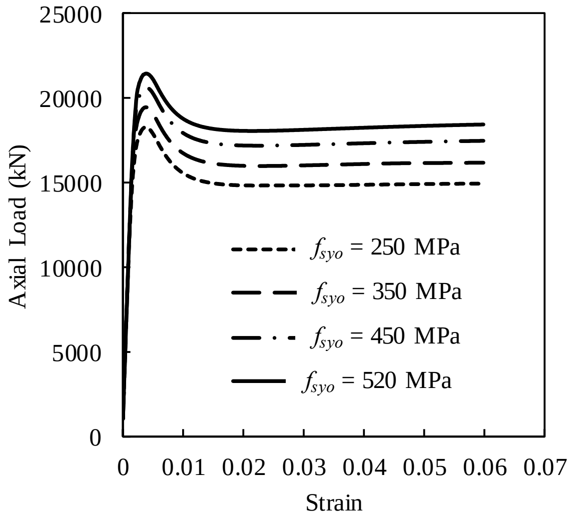

Fig. 19. Effects of the yield strength of the outer steel tube on the axial load-strain responses of CFDST short columns.

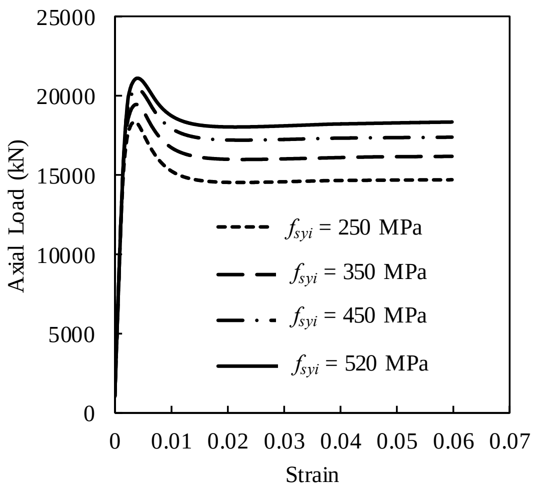

Fig. 20. Effects of the yield strength of the inner steel tube on the axial load-strain responses of CFDST short columns.

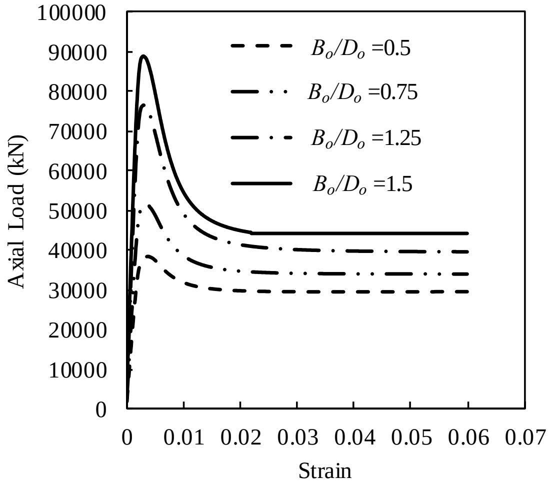

Fig. 21. Effects of the width-to-depth ratios on the axial load-strain responses of CFDST short columns.

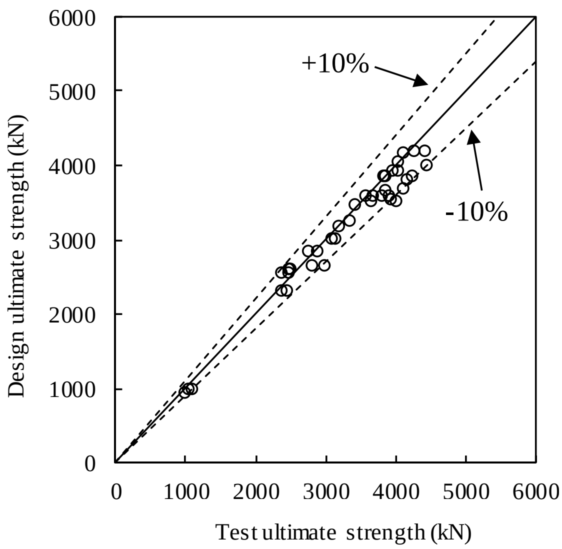

Fig. 22. Verification of the design model.